Segmental dynamics measured by quasi-elastic neutron scattering and ion transport in chemically-distinct polymer electrolytes

Katrina Irene S. Mongcopa,[†] Daniel A. Gribble,[†] Whitney S. Loo,[†] Madhusudan Tyagi,[‡, §] Scott A. Mullin, [#] and Nitash P. Balsara[*,†,▽,⊗]

[†]Department of Chemical and Biomolecular Engineering, University of California, Berkeley, Berkeley, California 94720, United States

[‡]National Institute of Standards and Technology Center for Neutron Research, Gaithersburg, Maryland 20899, United States

[§]Department of Materials Science and Engineering, University of Maryland, College Park, Maryland 20742, United States

[#]Seeo Inc., Hayward, California 94545, United States

[▽]Materials Sciences Division, Lawrence Berkeley National Laboratory, Berkeley, California 94720, United Sates

[⊗]Joint Center for Energy Storage Research, Lawrence Berkeley National Laboratory, Berkeley, California 94720, United States

Abstract

We investigate the segmental dynamics and ion transport in two chemically-distinct polymer electrolytes: poly(cyano 2-cyanoethyl acrylate) (PCEA) and poly(ethylene oxide) (PEO), and their mixtures with lithium bis-(trifluoromethane)sulfonimide (LiTFSI) salt. Quasi-elastic neutron scattering experiments reveal slow dynamics in PCEA/LiTFSI relative to that in PEO/LiTFSI, translating to monomeric friction coefficients that are orders of magnitude different. In spite of the enhanced salt dissociation in PCEA due to the presence of polar groups, ion transport is largely dominated by the effect of increased monomeric friction in the pure polymer. Conductivity in these systems is quantified through a simple expression combining salt dissociation, the monomeric friction in the pure polymer, and the effect of added salt on the monomeric friction.

TOC Graphic

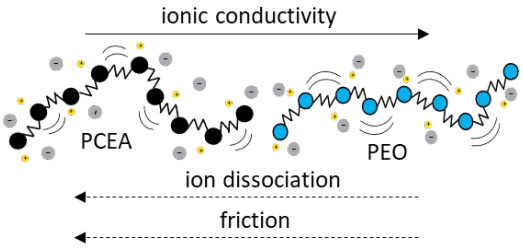

Introduction

There is growing interest in shifting towards solid polymer electrolytes to meet the demands for safe, high energy density rechargeable batteries. The current state-of-the-art lithium-ion battery consists of an organic liquid electrolyte, typically mixtures of alkyl carbonates and salts such as $LiPF_6$, through which lithium ions are shuttled back and forth between the electrodes during charge and discharge. However, the inherent flammability and incompatibility of liquid electrolytes with novel active materials have prompted the development of promising alternatives based on high molecular weight polymers.[1] Prototypical polymer electrolytes are mixtures of poly(ethylene oxide) (PEO) and lithium bis(trifluoromethane)sulfonimide (LiTFSI) salt.[2–4] Nitrile or cyano-based polymer electrolytes have also stimulated interest due to their high dipole moments and high dielectric constants, favoring interaction with lithium ions.[5]

An important prerequisite to the applicability of these polymer electrolytes is an understanding of the mechanism of ion transport in such systems. It is known that the dynamics of the polymer chains, to a large extent, influence ion conduction in these materials.[6,7] In previous work,[8] we quantified the underlying segmental dynamics in PEO/LiTFSI mixtures and established how it affects ionic conductivity. We extend this study by comparing the PEO/LiTFSI system to a chemically-distinct polymer electrolyte consisting of poly(2-cyanoethyl acrylate) (PCEA)/LiTFSI over a wide range of

salt concentrations, elucidating the effect of segmental dynamics on ionic conductivity in polymers with high dielectric constants.

Quasi-elastic neutron scattering (QENS) is a powerful tool for understanding the relaxation mechanisms of polymers in space and time.[9–11] In this work, we use QENS to investigate dynamics on length scales between 5 and 50 Å and time scales between 0.1 to 2 ns. Previous work has shown that the addition of salt slows down the polymer dynamics on these time- and length-scales.[8,12–14] The QENS data are used to determine the effect of added salt on the monomeric friction coefficient in both PCEA- and PEO-based electrolytes. We explore the relationships between this parameter and ionic conductivity in the two systems. Ion transport depends on both frictional effects and salt dissociation. Our analysis enables decoupling of these effects.

Experimental Methods

Synthesis of poly(2-cyanoethyl acrylate) (PCEA)

2-cyanoethyl acrylate (9.43 ml, 80 mmol) and acetone (32 ml) were combined in a round bottom flask equipped with a stir bar. 1-dodecanethiol (0.095 ml, 0.4 mmol) and AIBN (264 mg, 1.6 mmol) were then added to the flask, and the solution was sealed and bubbled under argon for 30 min. The solution mixture was placed in an oil bath at 60 °C and reacted for 5 hrs. The reaction mixture was then exposed to air and dropwise added to cold methanol. Further purification was performed by re-dissolving the solid in acetone, reprecipitating in methanol and drying under vacuum to afford a

colorless, sticky polymer. The resulting polymer (Figure 1) was characterized by size-exclusion chromatography (M_n = 10,700 g/mol, PDI = 1.203), NMR and FTIR, as presented in the Supporting Information.

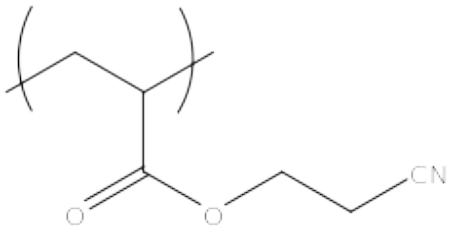

Figure 1. Structure of poly(cyanoethyl acrylate) (PCEA).

Materials and electrolyte preparation

The poly(ethylene oxide) had a molecular weight of 35 kg/mol and was obtained from Polymer Source. The LiTFSI salt was obtained from Novolyte. The materials were processed and the electrolytes were prepared according to Ref 15. All sample preparation was performed in an argon glovebox (MBraun) to minimize exposure to water and oxygen. All materials were initially dried under vacuum at 90 °C for at least 24 h prior to use. Polymer electrolytes were prepared by mixing the appropriate amounts of LiTFSI (Novolyte) and the polymer in anhydrous tetrahydrofuran to obtain the desired salt concentration (in molality). The solutions were allowed to mix for several hours at 65 °C to ensure complete mixing, after which the solvent was allowed to evaporate overnight. The polymer electrolytes were then dried at 90 °C under vacuum overnight to ensure complete solvent removal.

Electrochemical characterization

Ion transport properties were determined by performing electrochemical measurements on symmetric cells made of blocking

electrodes. Conductivity samples for PEO/LiTFSI and PCEA/LiTFSI were prepared by pressing the polymer into a 508 µm thick silicone spacer and sandwiching between two 200 µm thick stainless-steel electrodes. Nickel tabs were secured to the stainless-steel shims to serve as current collectors. The assembly was vacuum sealed in a laminated pouch material (Showa-Denko) prior to removal from the glovebox. Electrochemical impedance spectroscopy was performed within a frequency range of 1 MHz to 1 Hz and sinusoidal amplitude of 60 mV. The final electrolyte thickness was determined by subtracting the electrode thickness from the total cell thickness after the experiments were completed. Conductivity was then determined according to the equation,

$$\kappa = \frac{l}{A \bullet R_b} (1)$$

where l is the electrolyte thickness, A is the sample area and R_b is the bulk resistance determined from the low frequency minimum in the resulting Nyquist impedance plot.

Quasi-elastic neutron scattering

Quasi-elastic neutron scattering (QENS) samples were prepared by sandwiching a thin film of the polymer electrolyte between two pieces of aluminum foil and sealing in aluminum cans under a helium environment. Measurements were performed on the NG2 high-flux backscattering spectrometer (HFBS) at the NIST Center for Neutron Research. Data are collected over time scales ranging from 0.1 to 2 ns and reciprocal space

ranging from Q = 0.25 to 1.75 $Å^{-1}$, where Q is the magnitude of the scattering vector, Q. Experiments were performed at 90 ℃ and 120 ℃ for PEO/LiTFSI and PCEA/LiTFSI, respectively. We first performed the PEO/LiTFSI experiments and were hoping to perform experiments on PCEA/LiTFSI at 90 ℃. Unfortunately, we found that the dynamics in the PCEA system at 90 ℃ were too slow for the QENS experiment. We thus decided to examine the PCEA system at 120 ℃.

Results and Discussion

The dependence of conductivity, κ, on salt concentration (molality, m) for the PCEA/LiTFSI system at different temperatures is plotted in Figure 2. At all temperatures, the PCEA/LiTFSI system exhibits a monotonic increase in κ with increasing salt concentration before reaching a plateau at m = 0.9 mol/kg. The increase in conductivity is due to an increase in charge carrier concentration. However, the addition of salt slows down segmental motion which in turn impedes ion transport. The plateau at high salt concentrations is due to the balancing of these two competing effects. While κ increases with increasing temperature, the qualitative dependence of κ on salt concentration is unaffected.

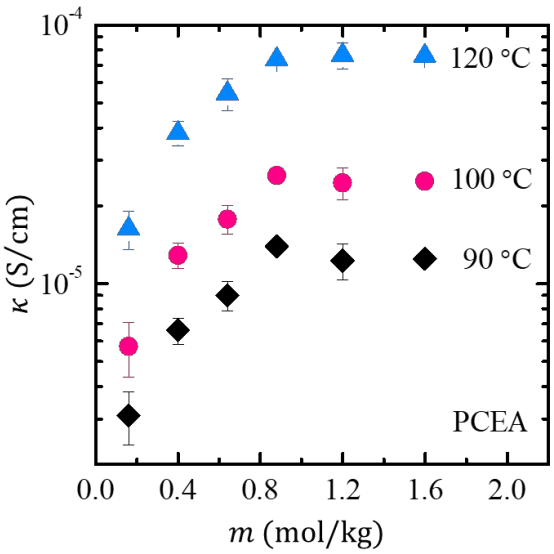

Figure 2. Conductivity, κ, of PCEA/LiTFSI measured at different temperatures using ac impedance spectroscopy, and plotted as a function of salt molality, m. Error bars represent the standard deviation of the measurements.

Figure 3 shows the dependence of κ on salt molality for PEO/LiTFSI and PCEA/LiTFSI at 90 °C. The molecular weights of both polymers are in the regime where ionic conductivity is not a function of molecular weight ($M_{n,PEO}$ = 35 kg/mol, $M_{n,PCEA}$ = 10 kg/mol).[16] The data obtained from PEO/LiTFSI is similar to PCEA/LiTFSI; conductivity of PEO/LiTFSI increases with increasing salt concentration and a plateau is observed when m>¿ 1.5 mol/kg. Across the entire salt concentration range investigated, the κ of PEO/LiTFSI is at least two orders of magnitude higher than that of PCEA/LiTFSI. In this work, we attempt to reconcile this difference by comparing the dissociation and friction in these chemically-distinct polymers. Friction is quantified using QENS.

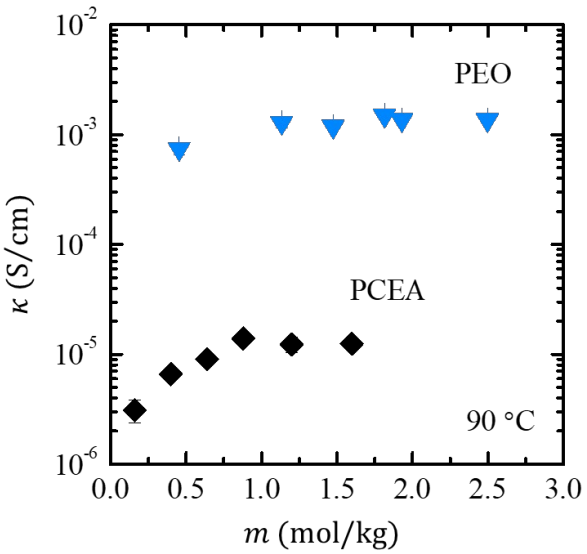

Figure 3. Conductivity, κ, of PEO/LiTFSI and PCEA/LiTFSI measured at 90 °C using ac impedance spectroscopy, and plotted as a function of molality, m. Error bars represent the standard deviation of the measurements.

QENS provides information on the dynamics in a sample by measuring the change in energy of the scattered neutrons, $\hbar\omega$.[17] Due to the large incoherent scattering cross section of hydrogen, the scattering intensity is primarily dominated by the motion of hydrogen atoms in the polymers (LiTFSI does not contain hydrogen atoms). The dependence of the normalized $S_{inc}(Q,\omega)$ on $\hbar\omega$ obtained at a representative scattering vector Q=¿ 0.62 Å^{-1} for PCEA/LiTFSI at 120 °C is shown in Figure 4a. The frequency-dependent data shown in Figure 4a is re-expressed in the time domain using a program provided by NIST (DAVE).[18] The same program also accounts for instrumental resolution. The output of this program is $S_{inc}(Q,t)$ which is related to the mean-square displacement of the hydrogen atoms, ¿$r^2(t)$>¿:

$S_{inc}(Q,t)$=exp¿

The dependence of r^2 on t was obtained from the data in Figure 4a and the results are shown in Figure 4b (Q=¿ 0.62 Å^{-1}). The data are in agreement with the expected Rouse scaling of r^2 $t^{1/2}$.[19,20] The solid lines in Figure 4b represent least squares fits through the data and are used to calculate the diffusion parameter, D_R=¿r^2>¿$t^{1/2}$. This parameter is plotted in Figure 4c as a function of Q. In theory,[21] D_R is expected to be independent of Q. The dashed lines in Figure 4c represent the average values of D_R obtained at the given salt concentrations. D_R generally decreases with increasing salt concentration, except for m = 0.4 mol/kg.

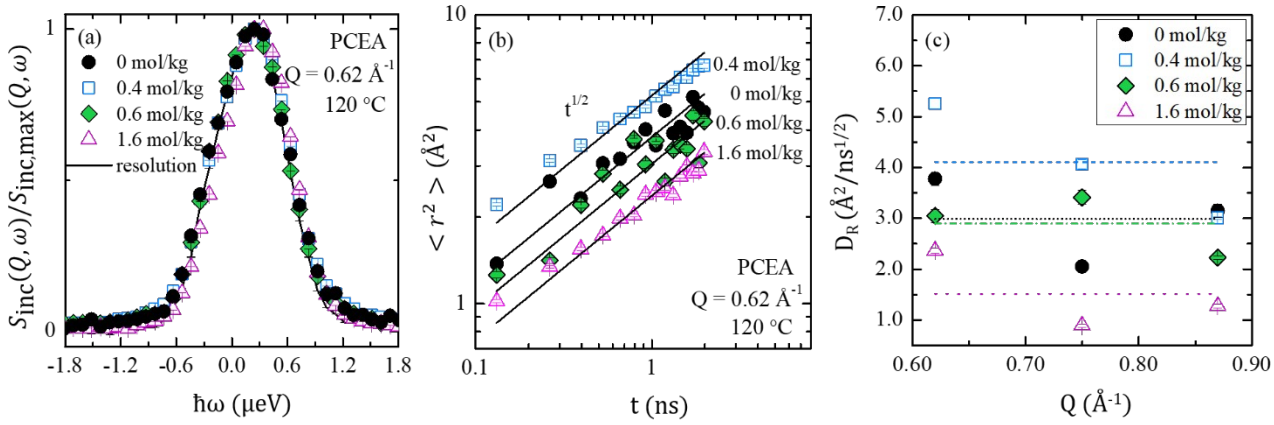

Figure 4. (a) Normalized incoherent structure factor, $S_{inc}(Q,\omega)/S_{inc,max}(Q,\omega)$, in the frequency domain, plotted as a function of energy, $\hbar\omega$, at Q = 0.62 Å^{-1} and 120 °C. The structure factor was measured by QENS. (b) Mean-square displacement, ¿r^2>¿, as a function of time, t, from QENS experiments at Q = 0.62 Å^{-1} with solid lines representing fits to the Rouse scaling, ¿r^2>¿ t$^{1/2}$. (c) Diffusion parameter, D_R, plotted as a function of Q for electrolytes with different salt concentrations expressed in molality. Dashed lines represent average values of D_R.

We use the Rouse model to relate D_R to the monomeric friction coefficient, ζ, according to equation 3,

$$\zeta = \frac{12 k_B T l^2}{D_R^2 \pi} \quad (3)$$

where l is the statistical segment length of the monomer unit. While explicit measurement of statistical segment length using small-angle neutron scattering for PEO as well as for PEO/LiTFSI mixtures has been reported in literature,[21,22] we are not aware of any reports of data for PCEA. It has been shown in Ref [23] that the statistical segment length of a wide variety of polymers is 6 Å when the monomeric reference volume is taken to be 0.1 nm^3. We therefore assume that l for PCEA and PEO is 6 Å,[23] and obtain the dependence of ζ on salt concentration using equation 3. The resulting plots of ζ versus salt concentration are shown in Figure 5. ζ is the average friction coefficient over the scattering vectors of $0.62<Q\left(\AA^{-1}\right)<0.75$. The data for the PEO/LiTFSI system are reproduced from Ref 8. It is clear that in both systems, ζ increases with salt concentration. However, the segmental dynamics in PCEA/LiTFSI at 120 °C is about a hundred times slower than that in PEO/LiTFSI at 90 °C. It is thus clear that the differences in conductivities between the two systems seen in Figure 3 is due, at least in part, to differences in segmental dynamics.

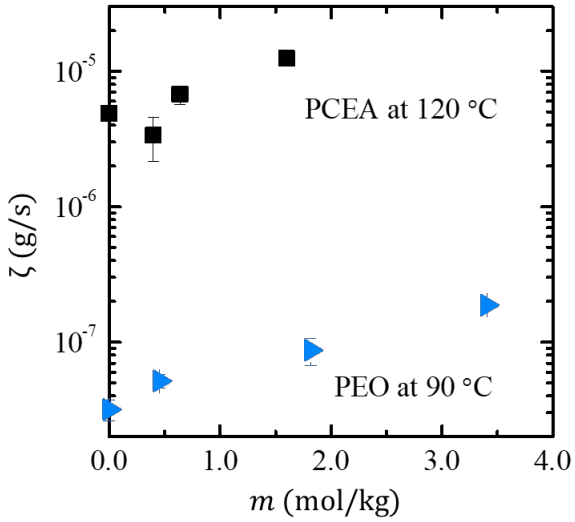

Figure 5. Average friction coefficient, ζ, of PCEA at 120 °C and PEO at 90 °C as a function of molality, m.

In Figure 6, we plot the normalized monomeric friction coefficient, $\zeta(m)/\zeta(0)$, as a function of salt concentration for PCEA. The monomeric friction coefficient increases exponentially with salt concentration; at $m=1.6\,kg/mol$, ζ is about a factor of 2.5 larger than that of neat PCEA. The dashed curve in Figure 6 is an exponential fit through the data which gives

$$\frac{\zeta(m_{PCEA})}{\zeta(0)}=\exp\left(\frac{m_{PCEA}}{1.72}\right) \quad (4)$$

In our analysis, a single parameter, M_f or the segment mobility factor, quantifies the slowing down of segmental dynamics due to the interactions between polymer chains and salt; for PCEA/LiTFSI at 120 °C, M_f = 1.72 mol/kg. More complex functional forms for this slowing down have been recently proposed in the literature.[24]

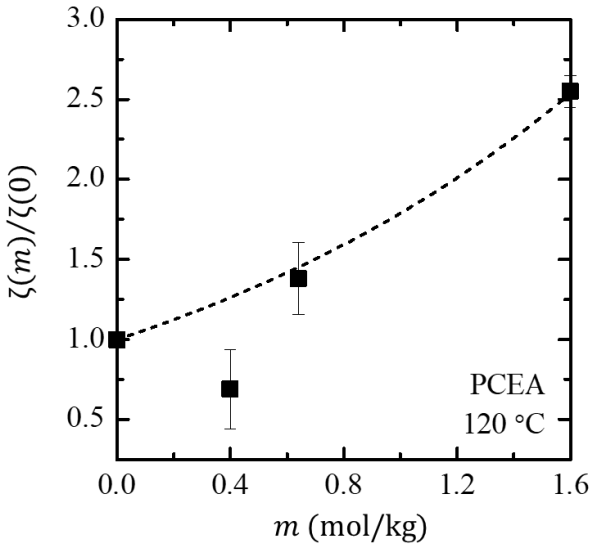

Figure 6. Normalized average friction coefficient, $\zeta(m)/\zeta(0)$, of PCEA at 120 °C as a function of molality, m. The dashed curve represents equation 4.

A similar relationship describes the effect of salt concentration on ζ in a PEO/LiTFSI system at 90 °C as presented in our previous work.[8] When the salt concentration is expressed in terms of molality, the expression for PEO/LiTFSI becomes

$$\frac{\zeta(m_{PEO})}{\zeta(0)}=\exp\left(\frac{m_{PEO}}{1.94}\right) \quad (5)$$

which gives M_f=1.94 kg/mol for PEO/LiTFSI at 90 °C.

It is instructive to examine the product $(\kappa\zeta)$ for the two electrolyte systems to quantify the effect of segmental dynamics on ion transport. If conductivity were only dependent on frictional effects, this product would be identical for the two electrolytes. In Figure 7, we plot $(\kappa\zeta)$ versus molality, m, for PCEA and PEO at 120 °C and 90 °C, respectively. In spite of the fact that the conductivity of PEO is much larger than that of PCEA, the product $(\kappa\zeta)$ is

only about an order of magnitude larger for PCEA across the entire salt concentration range.

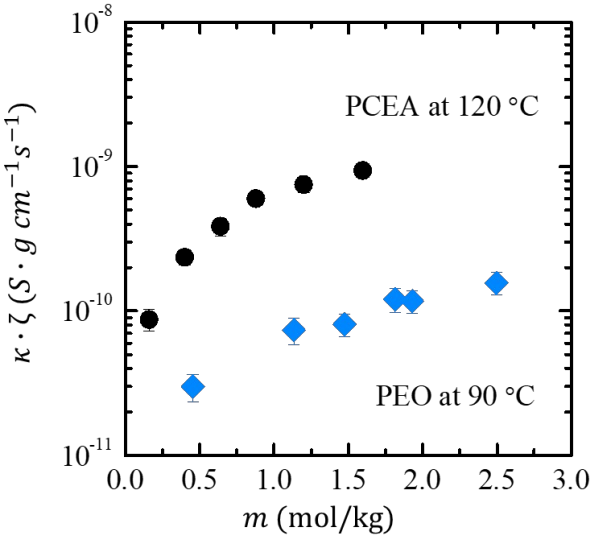

Figure 7. Product of conductivity, κ, and monomeric friction coefficient, ζ, plotted as a function of salt concentration for PCEA at 120 °C and PEO at 90 °C. ζ is determined using Eq. 4 and 5 for PCEA and PEO, respectively.

Ionic conductivity depends on three parameters: (1) salt concentration, (2) the extent of dissociation of the salt, and (3) frictional effects.[25–27] We present a simple expression that captures this dependence:

$$\kappa = \left(\frac{K}{\zeta(0)}\right) m \exp\left(\frac{-m}{M_f}\right) \quad (6)$$

where the parameter K reflects the extent of the salt dissociation. In our previous work,[8] we proposed that ionic conductivity is given by the product of a linear function of salt concentration and the exponential increase in friction captured by equations 4 and 5. The prefactor, $\left(\frac{K}{\zeta(0)}\right)$, in equation 6 is necessary for comparing chemically-distinct polymers to account for

differences in the dielectric constant of the polymers which will affect K, as well as differences in the monomeric friction coefficients in the absence of salt. We have already determined M_f for the two systems. We use the data in Figure 8 to determine K. The dashed curves in Figure 8 are fits of equation 6 through the data which give

$$\kappa_{PEO}=\left(\frac{5.75x10^{-11}}{3.18x10^{-8}}\right)m_{PEO}\exp\left(\frac{-m_{PEO}}{1.94}\right),(7)$$

¿

$$\kappa_{PCEA}=\left(\frac{6.47x10^{-10}}{4.88x10^{-6}}\right)m_{PCEA}\exp\left(\frac{-m_{PCEA}}{1.72}\right).(8)$$

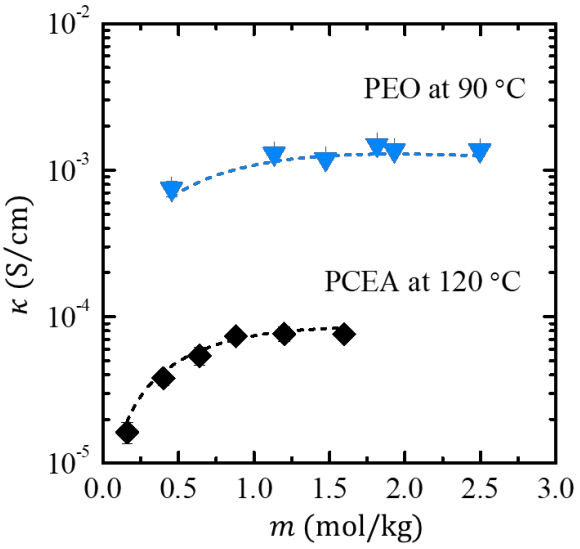

Figure 8. Conductivity, κ, of PEO at 90 °C and PCEA at 120 °C using ac impedance spectroscopy plotted as a function of salt concentration. The dashed curves represent equations 7 and 8 for PEO and PCEA, respectively.

In our analysis, the ionic conductivity of polymer electrolytes is governed by K, $\zeta(0)$, and M_f. In Table 1, we list these parameters for PEO and PCEA electrolytes. It is helpful to examine the ratios of these parameters when we compare electrolytes (see Table 1). The dissociation in PEO is

significantly worse than that in PCEA, $\frac{K_{PEO}}{K_{PCEA}}<1$. However, the monomeric friction in pure PEO is much lower than that of PCEA, $\frac{\zeta_{PEO}(0)}{\zeta_{PCEA}(0)}<1$. Surprisingly, the effect of added salt on friction, quantified by M_f, is similar in both systems, $\frac{M_{f,PEO}}{M_{f,PCEA}}\approx 1$. It is obvious that the increased dissociation seen in PCEA comes at a disproportionate cost of increased monomeric friction relative to PEO. The increased salt dissociation in PCEA is attributed to the presence of three polar sites on the monomer, C≡N, C¿O and –O– (Figure 1).[28–30] In contrast, the PEO monomer only contains one polar site, –O–.

Table 1. *K*, $\zeta(0)$, and M_f for PEO and PCEA.

	K	$\zeta(0)$	M_f
PEO at 90 °C	$5.75x10^{-11}$	$3.18x10^{-8}$	1.94
PCEA at 120 °C	$6.47x10^{-10}$	$4.88x10^{-6}$	1.72
PEO/PCEA	$8.89x10^{-2}$	$6.52x10^{-3}$	1.13

Conclusions

We have used QENS to quantify the effect of segmental dynamics in chemically-distinct polymer electrolytes. In the case of PCEA/LiTFSI, we found slower segmental dynamics relative to that of PEO/LiTFSI.[8] The Rouse model

allowed for the determination of the monomeric friction coefficient, which for PCEA/LiTFSI is orders of magnitude higher than that of PEO/LiTFSI. The dependence of ionic conductivity of polymer electrolytes on salt concentration is quantified by a simple expression (Eq 6) that contains three parameters, K, $\zeta(0)$ and M_f, quantifying salt dissociation, monomeric friction in the pure polymer, and the effect of added salt on monomeric friction. These parameters are given in Table 1. The introduction of polar groups in PCEA leads to significant enhancement of salt dissociation. Unfortunately, the accompanying effect of increased monomeric friction in the pure polymer dominates, resulting in diminished ion transport. The proposed framework is a simple starting point for quantifying the factors that govern ion transport in chemically-distinct polymer electrolytes.

Author Information

Corresponding Author

*(NPB) E-mail: nbalsara@berkeley.edu

Author Contributions:

The manuscript was written through contributions of all authors. All authors have given approval to the final version of the manuscript.

Notes:

The authors declare no competing financial interest.

The identification of any commercial product or trade name does not imply endorsement or recommendation by the National Institute of Standards and Technology.

Acknowledgements

This work was supported by the Bosch Energy Research Network grant. Access to the HFBS was provided by the Center for High Resolution Netron

Scattering, a partnership between the National Institute of Standards and Technology and the National Science Foundation under Agreement No. DMR-1508249. W.S.L. acknowledges funding from the National Science Foundation Graduate Student Research Fellowship DGE-1106400.

Supporting Information

Supporting information on the characterization of the poly(cyano 2-cyanoethyl acrylate) is provided.

List of Symbols

English

D_R	diffusion parameter (Å^2/ns$^{1/2}$)
K	dissociation constant
m	molality (kg/mol)
M_f	segment mobility factor
M_n	polymer molecular weight (kg/mol)
Q	scattering vector (Å$^{-1)}$
¿r^2>¿	mean-squared displacement (Å^2)
S_{inc}	incoherent structure factor
t	time (ns)

Greek

$\hbar\omega$	energy of scattered neutrons
κ	ionic conductivity (S/cm)
ζ	monomeric friction coefficient (g/s)

List of Abbreviations

AIBN	azobisisobutyronitrile
LiTFSI	lithium bis(trifluoromethane)sulfonimide salt
PCEA	poly(cyano 2-cyanoethyl acrylate)
PDI	polydispersity index

PEO	poly(ethylene oxide)
QENS	quasi-elastic neutron scattering

References

(1) Goodenough, J. B.; Kim, Y. Challenges for Rechargeable Li Batteries. *Chem. Mater.* **2010**, *22* (3), 587–603 DOI: 10.1021/cm901452z.

(2) Scrosati, B.; Vincent, C. a. Polymer Electrolytes: The Key to Lithium Polymer Batteries. *MRS Bull.* **2000**, *25* (March), 28 DOI: 10.1557/mrs2000.15.

(3) Mao, G.; Saboungi, M. L.; Price, D. L.; Armand, M. B.; Howells, W. S. Structure of Liquid PEO-LiTFSI Electrolyte. *Phys. Rev. Lett.* **2000**, *84* (24), 5536–5539 DOI: 10.1103/PhysRevLett.84.5536.

(4) Fenton, D. E.; Parker, J. M.; Wright, P. V. Complexes of Alkali Metal Ions with Poly(Ethylene Oxide). *Polymer (Guildf).* **1973**, *14* (11), 589 DOI: 10.1016/0032-3861(73)90146-8.

(5) Hu, P.; Chai, J.; Duan, Y.; Liu, Z. Progress in Nitrile-Based Polymer Electrolytes for High Performance Lithium Batteries. **2016**, 10070–10083 DOI: 10.1039/C6TA02907H.

(6) Shi, J.; Vincent, C. A. The Effect of Molecular Weight on Cation Mobility in Polymer Electrolytes. *Solid State Ionics* **1993**, *60* (1–3), 11–17 DOI: 10.1016/0167-2738(93)90268-8.

(7) Bresser, D.; Lyonnard, S.; Iojoiu, C.; Picard, L.; Passerini, S. Decoupling Segmental Relaxation and Ionic Conductivity for Lithium-Ion Polymer Electrolytes. *Mol. Syst. Des. Eng.* **2019** DOI: 10.1039/c9me00038k.

(8) Mongcopa, K. I. S.; Tyagi, M.; Mailoa, J. P.; Samsonidze, G.; Kozinsky, B.; Mullin, S. A.; Gribble, D. A.; Watanabe, H.; Balsara, N. P. Relationship between Segmental Dynamics Measured by Quasi-Elastic Neutron Scattering and Conductivity in Polymer Electrolytes. *ACS Macro Lett.* **2018**, *7* (4), 504–508 DOI: 10.1021/acsmacrolett.8b00159.

(9) Richter, B. D.; Ewzn, B. Neutron Spin-Echo Investigations on the Dynamics of Polymers. *Appl. Cryst* **1988**, *21*, 715–728 DOI: 10.1107/S002188988800487X.

(10) Zorn, R.; Arbe, A.; Colmenero, J.; Frick, B.; Richter, D.; Buchenau, U. Neutron Scattering Study of the Picosecond Dynamics of Polybutadiene and Polyisoprene. *Phys. Rev. E* **1995**, *52* (1), 781–795 DOI: 10.1103/PhysRevE.52.781.

(11) Bée, M. Localized and Long-Range Diffusion in Condensed Matter: State of the Art of QENS Studies and Future Prospects. *Chem. Phys.* **2003**, *292* (2–3), 121–141 DOI: 10.1016/S0301-0104(03)00257-X.

(12) Mao, G.; Saboungi, M. L.; Price, D. L.; Armand, M.; Mezei, F.; Pouget, S. α-Relaxation in PEO-LiTFSI Polymer Electrolytes. *Macromolecules* **2002**, *35* (2), 415–419 DOI: 10.1021/ma010108e.

(13) Frischknecht, A. L.; Paren, B. A.; Middleton, L. R.; Koski, J. P.; Tarver, J. D.; Tyagi, M.; Soles, C. L.; Winey, K. I. Chain and Ion Dynamics in Precise Polyethylene Ionomers. *Macromolecules* **2019** DOI: 10.1021/acs.macromol.9b01712.

(14) Fullerton-Shirey, S. K.; Maranas, J. K. Effect of LiClO 4 on the Structure

and Mobility of PEO-Based Solid Polymer Electrolytes. *Macromolecules* **2009**, *42* (6), 2142–2156 DOI: 10.1021/ma802502u.

(15) Timachova, K.; Watanabe, H.; Balsara, N. P. Effect of Molecular Weight and Salt Concentration on Ion Transport and the Transference Number in Polymer Electrolytes. *Macromolecules* **2015**, 151019083859005 DOI: 10.1021/acs.macromol.5b01724.

(16) Teran, A. a.; Tang, M. H.; Mullin, S. a.; Balsara, N. P. Effect of Molecular Weight on Conductivity of Polymer Electrolytes. *Solid State Ionics* **2011**, *203* (1), 18–21 DOI: 10.1016/j.ssi.2011.09.021.

(17) Jobic, H.; Renouprez, A.; Bee, M.; Poinsignon, C. Quasi-Elastic Neutron Scattering. *J. Phys. Chem.* **1986**, *90*, 1059–1065 DOI: 10.1063/1.3592560.

(18) Azuah, R. T.; Kneller, L. R.; Qiu, Y.; Tregenna-Piggott, P. L. W.; Brown, C. M.; Copley, J. R. D.; Dimeo, R. M. DAVE: A Comprehensive Software Suite for the Reduction, Visualization, and Analysis of Low Energy Neutron Spectroscopic Data. *J. Res. Natl. Inst. Stand. Technol.* **2009**, *114* (6), 341 DOI: 10.6028/jres.114.025.

(19) Niedzwiedz, K.; Wischnewski, A.; Monkenbusch, M.; Richter, D.; Genix, A. C.; Arbe, A.; Colmenero, J.; Strauch, M.; Straube, E. Polymer Chain Dynamics in a Random Environment: Heterogeneous Mobilities. *Phys. Rev. Lett.* **2007**, *98* (16), 1–4 DOI: 10.1103/PhysRevLett.98.168301.

(20) Brodeck, M.; Alvarez, F.; Arbe, A.; Juranyi, F.; Unruh, T.; Holderer, O.; Colmenero, J.; Richter, D. Study of the Dynamics of Poly(Ethylene

Oxide) by Combining Molecular Dynamic Simulations and Neutron Scattering Experiments. *J. Chem. Phys.* **2009**, *130* (9) DOI: 10.1063/1.3077858.

(21) Niedzwiedz, K.; Wischnewski, A.; Allgaier, J.; Richter, D. Chain Dynamics and Viscoelastic Properties of Poly (Ethylene Oxide). *Macromolecules* **2008**, *41* (13), 4866–4872.

(22) Loo, W. S.; Mongcopa, K. I.; Gribble, D. A.; Faraone, A. A.; Balsara, N. P. Investigating the Effect of Added Salt on the Chain Dimensions of Poly(Ethylene Oxide) through Small-Angle Neutron Scattering. *Macromolecules* **2019**, *52*, 8724–8732 DOI: 10.1021/acs.macromol.9b01509.

(23) Eitouni, H. B.; Balsara, N. P. CHAPTER 19 Thermodynamics of Polymer Blends. *Phys. Prop. Polym. Handb. 2e* **2006**, 339–356 DOI: 10.1007/978-0-387-69002-5_19.

(24) Webb, M. A.; Yamamoto, U.; Savoie, B. M.; Wang, Z. G.; Miller, T. F. Globally Suppressed Dynamics in Ion-Doped Polymers. *ACS Macro Lett.* **2018**, *7* (6), 734–738 DOI: 10.1021/acsmacrolett.8b00237.

(25) Webb, M. A.; Jung, Y.; Pesko, D. M.; Savoie, B. M.; Yamamoto, U.; Coates, G. W.; Balsara, N. P.; Wang, Z. G.; Miller, T. F. Systematic Computational and Experimental Investigation of Lithium-Ion Transport Mechanisms in Polyester-Based Polymer Electrolytes. *ACS Cent. Sci.* **2015**, *1* (4), 198–205 DOI: 10.1021/acscentsci.5b00195.

(26) Borodin, O.; Smith, G. D. Mechanism of Ion Transport in Amorphous

Poly(Ethylene Oxide)/ LiTFSI from Molecular Dynamics Simulations. *Macromolecules* **2006**, *39* (4), 1620–1629 DOI: 10.1021/ma052277v.

(27) Devaux, D.; Bouchet, R.; Glé, D.; Denoyel, R. Mechanism of Ion Transport in PEO/LiTFSI Complexes: Effect of Temperature, Molecular Weight and End Groups. *Solid State Ionics* **2012**, *227*, 119–127 DOI: 10.1016/j.ssi.2012.09.020.

(28) Saito, Y.; Hirai, K.; Murata, S.; Kishii, Y.; Kii, K. Ionic Diffusion and Salt Dissociation Conditions of Lithium Liquid Crystal Electrolytes. **2005**, 11563–11571.

(29) Sai, R.; Ueno, K.; Fujii, K.; Nakano, Y.; Shigaki, N.; Tsutsumi, H. And Transport Properties of Polyoxetane-Based. *Phys. Chem. Chem. Phys.* **2017**, *19*, 5185–5194 DOI: 10.1039/C6CP08386B.

(30) Sai, R.; Ueno, K. Properties in Polyoxetane-Based Polymer. *RSC Adv.* **2017**, *7*, 37975–37982 DOI: 10.1039/C7RA07636C.